Toward Predicting Filtration and Separation: Progress & Challenges

Andreas Wiegmann, Stefan Rief, Arnulf Latz and Oleg Iliev
Fraunhofer Institut für Techno- und Wirtschaftsmathematik,
Fraunhofer Platz 1, 67663 Kaiserslautern, Germany

ABSTRACT

The need for correctly predicting filtration and separation processes is greater than ever. New legislation, new materials, globalization and short development cycles require deeper understanding than before. Computer Simulations are a recent and efficient way to gain knowledge regarding filtration. But modeling and simulation efforts face serious difficulties in their quest to complement experiment / observation and theory. Filtration is a phenomenon determined by multiple scales. They range from the flow regime around a moving vehicle to the atomic regime of adhesion forces between dust particles and an electrically charged filter medium. Fortunately, powerful computers, sophisticated models and new experimental equipment are available. Desktop computers with lots of memory and several fast CPUs, three-dimensional filter media models combined with SEM and µCT images are some of the exciting developments that allow work today that was unthinkable in the past. We present examples how filter media models, filter process models, CFD and statistics can provide insights into filtration from the practical and the academic point of view.

KEYWORDS

Filtration, Simulation, Software, Multi-phase Modeling, Micro Scale Processes, Filter Media, Filter Performance.

1. Introduction

Particle Filtration is a highly complex phenomenon that poses countless challenges to modeling and simulation, most notably through the large differences in scales that come into play. Figure 1 illustrates the scales and applications where these scale considerations might arise from.

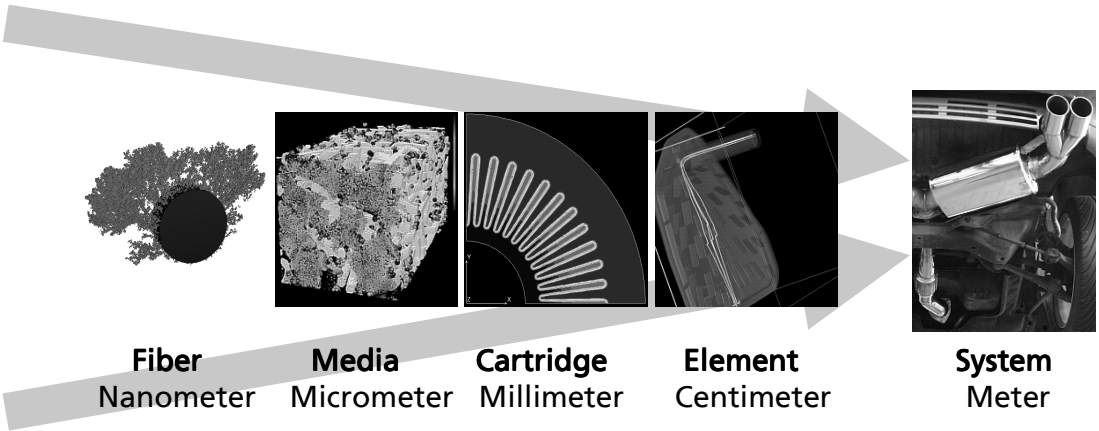

Figure 1: *Scales of filtration* considered in this work range from nano- to millimeters.

Some fluid (i.e., gas or liquid) transports the particles to the filter and through the filter media. The simulation of this fluid flow must be considered as two separate tasks. In the free flow up to the filter, the main concerns are the lowest possible pressure drop, equal distribution of particles to the filter, and the handling of the physical properties of the flow, for example turbulence. Within the filter media, the challenges lie in the facts that the precise geometry of the domain is usually not known and in the need to impose boundary conditions on the very complex boundaries of the flow domain. When particles are considered in this system, one finds that they interact with the fluid and with each other while in flight, and then also with the filter media and previously deposited particles via collisions. The shapes of the particles are not known, the adhesion or stickiness between particles and between particles and filter media are not known. Additional forces such as electric charges may have to be considered, yet neither the charges on the particles nor those on the filter media are known. When the force exerted by the flow becomes too large, or the direction of the flow is reversed (pulse cleaning), particles that were previously deposited may come loose again and break of in larger chunks. And all of these effects happen on scales from about 50 nanometers to several meters, from the smallest particles to the length of the exhaust system of a vehicle. So, from a simulation view point, particle filtration simulation poses three different types of difficulties:

1. The process is not completely understood.
2. The process is understood, but its parameters are not known.
3. The process and its parameters are known, but proper modeling would overwhelm the computational resources.

Effect / Scale	Geometric Structures	Filtration Physics	Software Considerations
Nanometer	Nano fibers Soot-cake formation Membranes	Slip flow Cunningham Adhesion Restitution	Millions of particles Very large domains Parallel computing Local coarsening
Micrometer	Nonwoven Packed beds Woven Filter cake	Nonwoven Interception Impaction Diffusion Electric charges Resolved Clogging	Randomness Navier-Stokes-Brinkman Effective soot cake Collision detection Bounce handling
Millimeter	Pleat shape Support structures CAD	Deformation Effective clogging Porous media	Track particles / concentrations Incorporate measured data Filter efficiency & life time

Table 1: Topics touched in this overview.

Progress is made with respect to all three of the above. A basic ingredient for this progress is the availability of new hardware. µCT or Micro Computer Tomography gives unprecedented insights into the three-dimensional structure of filter media. With this new data, it is possible to create sophisticated computer models of the filter media that ultimately allow the design of the filter media for specific applications. ATM or atomic force microscopy determines the adhesion forces between different materials. Such data is essential in the regime where some but not all colliding particles get collected. And last but not least, the progress in computer hardware, where PC can be spelled these days as *Personal Cluster*, has made possible detailed three-dimensional computations that were unconceivable only 5 years ago.

Besides the progress in hardware, also new models and new algorithms contribute to the progress in filtration simulation. Most notable for the models are the influence of electric fields in air filtration, stochastic geometry models for random filter media, incorporation of slip flow, treatment of particle collisions and bounce, subscale models of filter cake as porous media and the introduction of the Stokes-Brinkman equations for handling regimes of free and porous media flow that are so dominant in filtration applications. On the simulation side, the parallelization of the flow solvers and the ode tracking codes, task automation, handling and result extraction from massive result data sets and vastly improved pre- and post-processing capabilities are available today.

Table 1 gives an overview over the various scales and effects that are considered. The topics are grouped according to the three scales nanometer range, micrometer range and millimeter range, and according to whether they are a geometric aspect, filtration phenomenon, or simulation issue.

2. Filter and filter media simulation

Direct numerical simulation is based on realistic three dimensional geometric models of the filter and the filter media [5]. To validate the simulation, existing objects must be imported into the computer. CAD data sets are commonly available for the filter, while for the filter media, usually microscopy, SEM or µCT images may be available. The domain of interest is partitioned into small cells, the computational grid, to perform the simulations. The fundamental approach in the present work is to use a special 3D-image, a 3D-structure, for short **structure**, also as the computational grid: it is always a 3D rectangular array of typically between 1 million and 100 million cubic cells. The simplification of a structure compared to a 3D-image is the number of colors. Structures often contain only 2 colors, usually less than 10. Colors represent different materials and their properties, e.g. pores, polyester, ceramics, warp or weft wires, etc. All representations, µCT, CAD or analytic descriptions, get converted into structures.

Structure generators create structures of filter media based on analytic or statistical descriptions. Even designs that do not exist in reality can be considered and compared. The next paragraphs describe the principles behind several generators.

The fact that structures are simplified images has one further advantage besides the automatic grid generation. Images can be directly displayed and compared with images of the real objects. We distinguish 2D slice visualization, 2½D SEM

visualization and 3D visualization. All images below are created with the simulation software GeoDict, [18], unless otherwise noted.

2.1 *Nonwoven filter media*. The nonwoven structure generator takes 3 basic input parameters. They are the porosity of the nonwoven, the fiber diameter and a parameter describing the probabilities of the fiber directions, relating the through-plane to the in-plane component of the fibers [15]. On top of that, also the fiber's cross-sectional shape, fiber length, fiber mix, etc., help to completely characterize many synthetic fibers. The generator works by randomly picking positions and directions for the fibers with appropriately defined probability densities, and then placing the fibers in the initially empty structure that later represents the nonwoven.

Thus, besides the fibers also the size of the initially empty structure must be selected. For filtration applications, the through-plane direction is ideally completely covered. For the two lateral directions, large enough in-plane cutout lengths must be considered so that the computed pressure drop, filter efficiency and filter life time are representative. A simple way to test this representativeness is that the results should not change significantly if the fiber generator is started again with a different sequence of random numbers drawn from the same distributions as before.

Figure 2 illustrates the effect of the anisotropy parameter. The value 100 leads to fibers aligned almost perfectly in the plane, on the left. The smaller anisotropy parameter 7 leads to the orientation shown on the right, where fibers have a clear out-of-plane component. Each structure consists of 1000 x 1000 x 400 cells and requires 200 MB of memory. The generation takes about 10 seconds on a laptop. Here, the resolution was 1 µm so that 5 micron fibers appear as 5 grid cells.

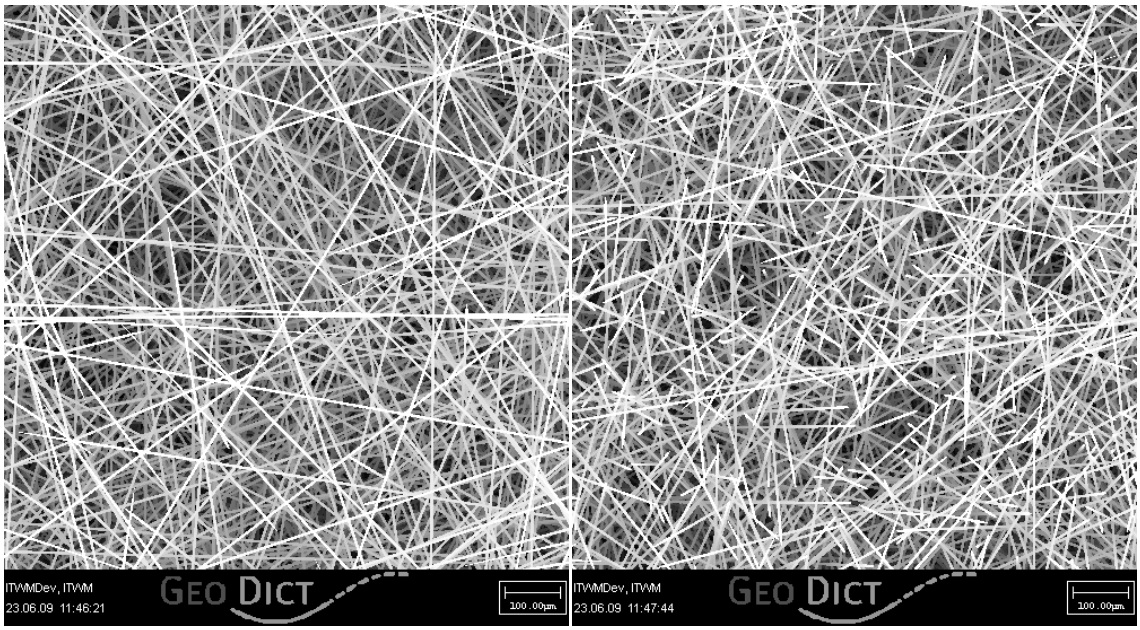

a) b)

Figure 2: SEM visualization of 8 volume percent 5 micron fibers at anisotropy 100 (left) and at anisotropy 7 (right), following [16].

2.2 *Woven filter media*. The woven structure generator applies both to textiles and metal wire meshes and takes as basic input the weave type, aperture and thread thicknesses or wire thicknesses. For textiles, both mono-filaments and multi-filaments

are possible. On top of that, additional options exist regarding the crank, broadening, lateral deformations etc. Similar to the nonwoven structure generator, also the woven structure generator starts with an initially empty structure and places threads or wires in selected cells. Different from nonwoven, woven are in principle deterministic, that is, threads or wires are always in the same position. However, in real production processes some randomness or tolerances occur – hence also the woven generator relies on a random number generator, for example to place the individual filaments in a multi-filament textile – see Figure3.

For woven, the size of the structure is determined by the textile parameters. A single copy of the pattern is representative of the woven and creates the lowest computational effort. The second factor determining this effort is the resolution. The smallest cross sectional dimension should be resolved by 5-6 grid cells, so that 10 micron filaments mandate 1.6 micron resolution and the pattern on the left of Figure 3 requires about 510 x 510 x 260 grid cells.

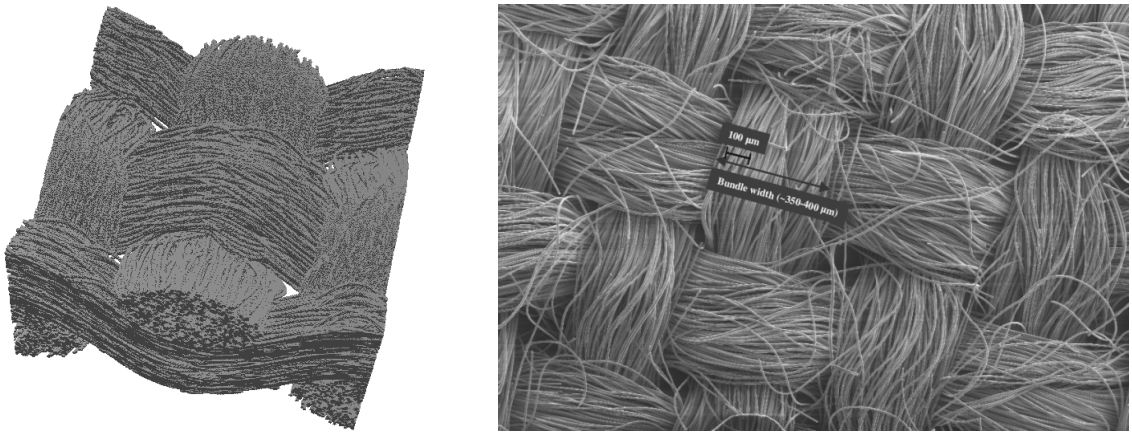

a) b)

Figure 3: 3D Visualization of a generated structure (a) and SEM of a carbon fiber multi-filament woven (b, courtesy of Jeff Gostick, University of Waterloo).

2.3 *Sintered filter media.* The generation of sintered structures occurs in two steps: first, a random object generator is used to create ellipsoids, cylinders and other basic geometric shapes. The positions, sizes and shapes are random, from pre-defined distributions. This is done recursively. Large ellipsoids are generated to represent large pores. Then the complement of the large ellipsoids is filled with smaller ellipsoids that represent the initial grains of the sinter structure. For the small grains, we look at the shape and size distributions of the grains of the real material and try to match these distributions. During the second step, morphological operations [13] are applied to generate the sinter necks. Iteratively using the operations dilatation and erosion creates exactly the intended connectivity.

Figure 4 shows binarized SEM images of 3 existing ceramics and cross section images of generated 3D structures that mimic these existing ceramics.

2.4 *Packed filter media*. Several methods exist to create packed filter media. One way is deposition of arbitrary objects with sideways motion and rotation upon collision with previously deposited objects. In this mode, the packing density cannot be prescribed, but arbitrary objects are possible. Collisions between objects are detected by discretizing the deposited objects into a fixed, initially empty structure,

and binarizing the moving objects temporarily on that same grid. The accuracy of the collision detection is thus limited by the size of its cubic cells used in the structure. It is possible to describe two types of container to be packed: the bottom is always a solid wall, but the side walls can be solid or periodic. Periodicity means that objects leaving on one side enter again through the opposite side.

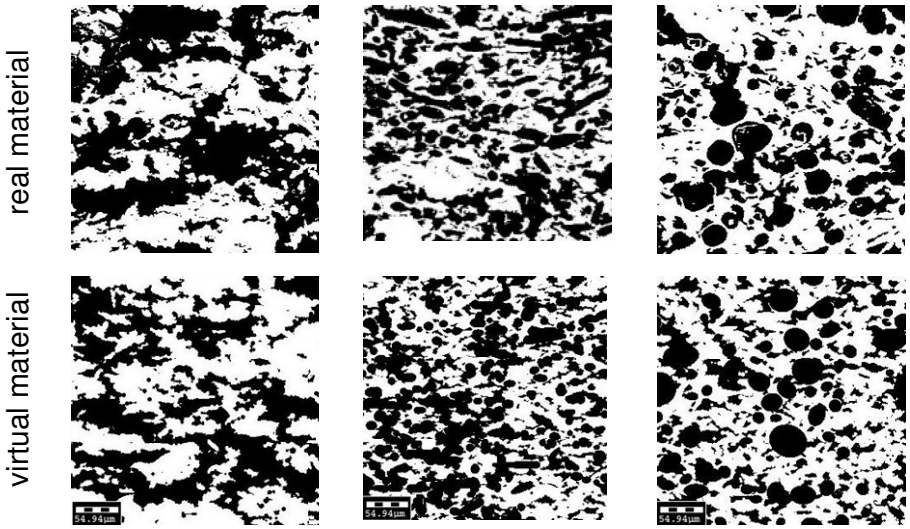

Figure 4: Binarized SEM images of real sintered materials and 2D cross section images of 3D generated structures. From [12].

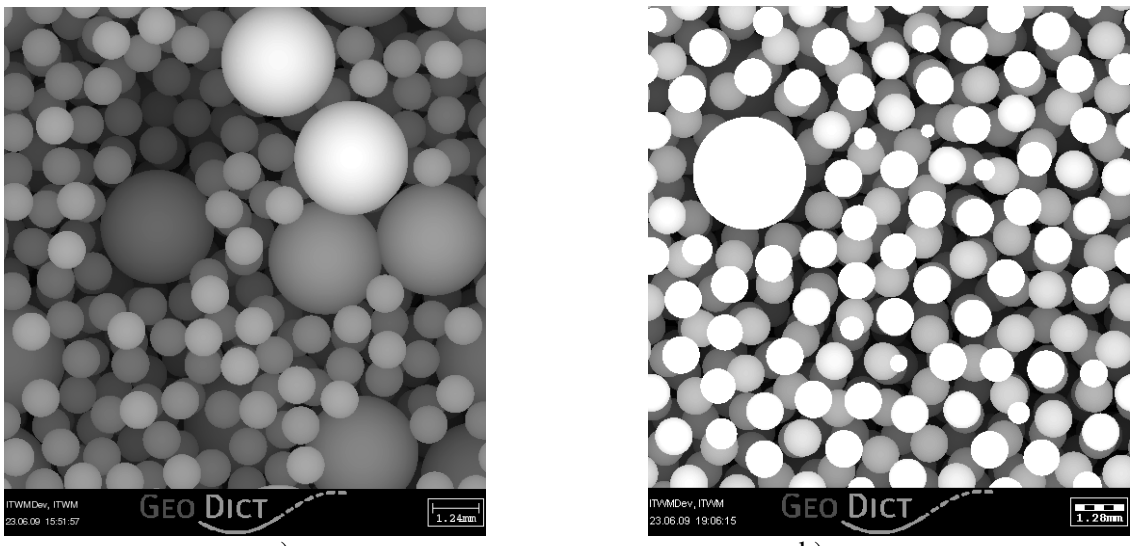

a) b)

Figure 5: Generated SEM images of packed spheres (solid volume fraction 0.64, a) and floating spheres (solid volume fraction 0.3, b). Size distributions are 3-1 at 50 – 50 relative volume percent (a) and 90-10 relative volume percent (b).

The second approach under consideration is the force-biased algorithm [1] for sphere packing. It works for spherical objects with varying sizes. Structures are always generated as cubes that are periodic in all three directions. The algorithm works by putting small spheres with correct distribution of relative sizes into the unit box. Then, spheres move around under repelling forces between them. After some time, their sizes are increased simultaneously by the smallest factor so that two of the spheres

touch. These steps are repeated until the desired density is reached or no more progress can be made. Finally, the spheres and domain are scaled up so that the spheres have the specified diameters. So, the size of the domain cannot be prescribed but results from the number of spheres and achieved packing density. The resolution can be selected independently from the sphere sizes and packing density. The tightest packing densities that are achievable with this method are about 65% of the volume for uni-modal distributions and slightly higher for variable sphere size distributions.

Figure 5 shows sphere packings with solid volume fractions of 0.64 and 0.30, respectively for spheres with 3-1 bi-modal size distributions at 50-50 volume percent and 10-90 volume percent.

2.5 *Filter cakes as porous media*. Particles cannot be represented on the computational grid when they are smaller than the resolution. When these particles deposit close to each other, they are modeled as porous media.

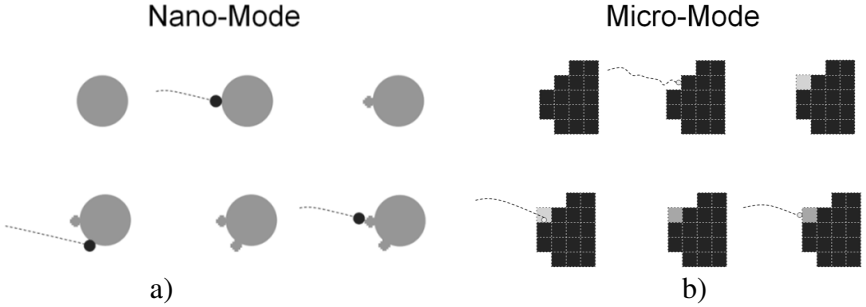

Figure 6: In nano-mode, (a), particles are resolved by the grid. Later particles deposit on previously deposited ones just like on the filter media. In micro-mode, (b), particles are smaller than the grid size and create porous cells that can get denser and less permeable as particles deposit. Ultimately, these cells become full and impenetrable and later particles deposit on the surfaces of such cells.

The parameters of this process are computed by detailed simulations (nano-mode, figure 6 left) that resolve the particles, but cover only a small portion of the filter media, such as for example a single fiber. The packing density and permeability of the deposited particles are computed. In general, these parameters are functions of the flow velocity, particle size distribution, etc., etc. The results from the detailed simulations then enter into simulations that do not resolve the particles but cover a representative portion of the media (micro-mode, Figure 6 right). On this scale, the porous media initially becomes denser as particles enter the cells. Once cells are considered full they become impenetrable for further particles while still being permeable for the flow calculations. A typical achievable solid volume fraction for depositing soot is 0.23.

2.6 *Pleat model for* c*artridge filters*. When the effects of the pleat shape, height and width must be considered, another scale comes into play. On this scale, the filter media is modeled as homogenized cells with so-called *effective* properties. The most important such property is the permeability. It may be set separately for each layer of a filter media [20]. Another question of wide interest is the influence of support structures on the pressure drop across a pleated filter. Such structures serve to keep the outflow region of the pleat open which is necessary not to invoke undue pressure

increase on the overall pressure drop [19]. If done well, the support structures may lower the initial pressure drop by as much as 40% if used appropriately. In the example in Figure 7 (left), a woven wire mesh in light gray is used to keep the pleated filter media (shown in darker gray) apart. The flow is from the back to the front, i.e. the view is into the outflow region with the supporting mesh inside it. The difference between light and dark zones is that the light ones are solid or impermeable obstacles, while the dark regions are permeable.

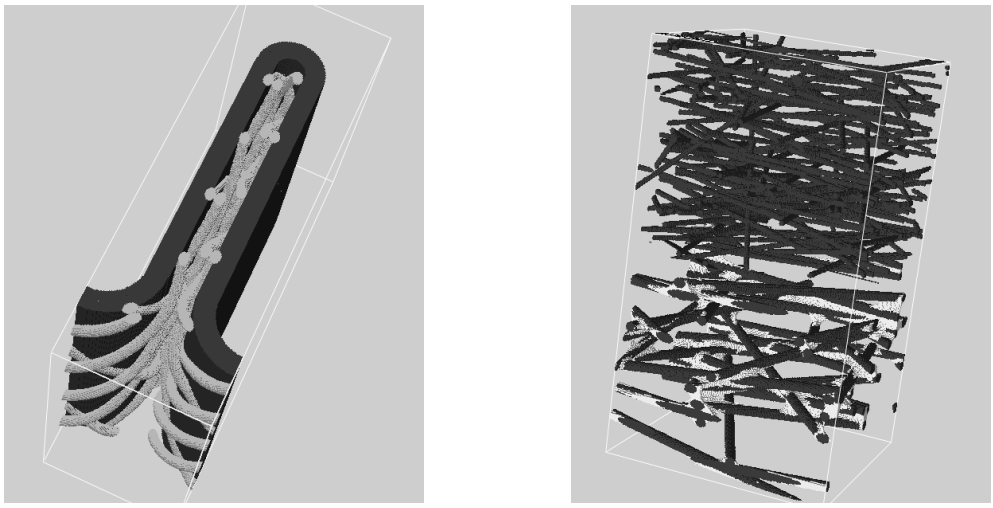

a) b)

Figure 7: Single pleat with woven support as used in oil filtration (a). Two layers of solid volume fraction 0.05, upper with 5 µm fibers, lower with 10 µm fibers with binder in lighter color (b).

2.7 *Layered media and binder*. Real filter media may incorporate multiple layers and may be bonded by a binder. To get realistic filtration simulation results, both features are incorporated into the models. Multiple layers can be modeled by creating a layer at a time and then merging the two or more layers into a single structure. Binder can be introduced using morphological operations [10]. The morphological closure with a given radius tends to create virtual binder just in the locations where the binder is also collected in reality – at the crossing points of fibers.

Figure 7 (a) illustrates the layer and binder models. It shows a two-layered media where the upper layer has finer fibers and a lower porosity. The lower layer has bigger fibers, a higher porosity, and contains binder at the fiber crossing points.

2.8 *Validation of virtual structures.* The first purpose of virtual structures is to reproduce existing media. To measure the quality of reproduction, several measures are used. If 2D microscopic images or scanning electron microscope (SEM) images or 3D tomography data of a sample are available, then this information can be used to compute and compare various geometrical properties like porosity, cord length distributions, pore size distributions, specific surface area, anisotropies, etc. [2]. If 3D data is provided and the structure is regular as is the case for woven structures, then the 3D images can be compared directly [7]. This comparison is illustrated in Figure 8, where the difference between an image of a real metal wire mesh and a virtual metal wire mesh is shown.

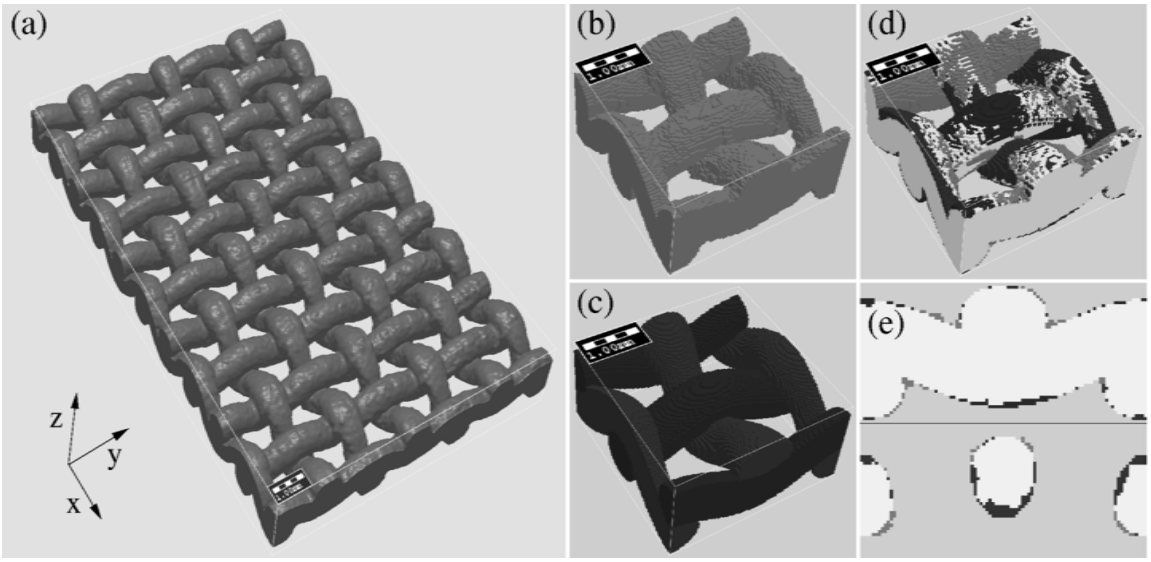

Figure 8: Tomography of a metal wire mesh and comparison with a virtual structure. (a), (b): Tomography, where (b) shows one repetitive unit. (c): Virtually generated repetitive unit. (d), (e): Comparison between tomography and generated structure. (d) shows a 3D image and (e) shows 2D cross sections. From [7].

In industry, flow resistivity tests of porous samples are standard. Moreover, flow simulations in typical porous media regimes, i.e. slow flow regimes are very reliable. Hence, measured and computed flow properties such as flow resistivity, permeability or pressure drop for given flow velocity can be compared reliably and provide meaningful results.

3. Filtration simulation

Once the filter media model is accepted, filtration simulation poses increasingly difficult tasks. The challenges range from the geometric characterization of pores through the computation of the pressure drop all the way to simulating filter efficiency and filter life time.

3.1 *Computation of the largest through pore.* For metal wire meshes, the prediction of absolute filter fineness is of interest. It corresponds to the largest sphere that may be pushed through the filter media in the direction of the flow. Figure 9 (left) illustrates this procedure by showing the path that a largest sphere takes through a Dutch weave metal wire mesh, or largest through pore, LTP. Our industrial partners assure us that the agreement of predicted and measured absolute filter fineness for such media is great [8]. Several other pore size measures can be simulated such as porosimetry and porometry [2].

All pore size measures are based on the computation of the Euclidean Distance transform (EDT) of the structure – it associates with every empty cell its distance from the nearest solid cell, for solid cells the distance defaults to zero. Fortunately, a very efficient algorithm for the EDT is available from the medical imaging literature [14]. The main point is to avoid the computation of the distance from every empty to every solid cell because this would scale with the square of the total number of cells and take extremely long for realistic pictures. To compute the LTP, a second, computationally even more demanding sub-problem arises: One must find the path

through the empty cells of the filter media so that the minimum of all distances from the solid cells along this path is maximized. Again, fortunately a very efficient algorithm is available for the computation of shortest paths along weighted graphs [4]. The main point is to avoid the computation of all possible paths, again for the sake of time and memory spent for realistic models of filter media. Instead, a small list of candidates is kept on a sorted heap. The algorithm runs twice, starting on the two faces, to make sure it finds the shortest possible LTP.

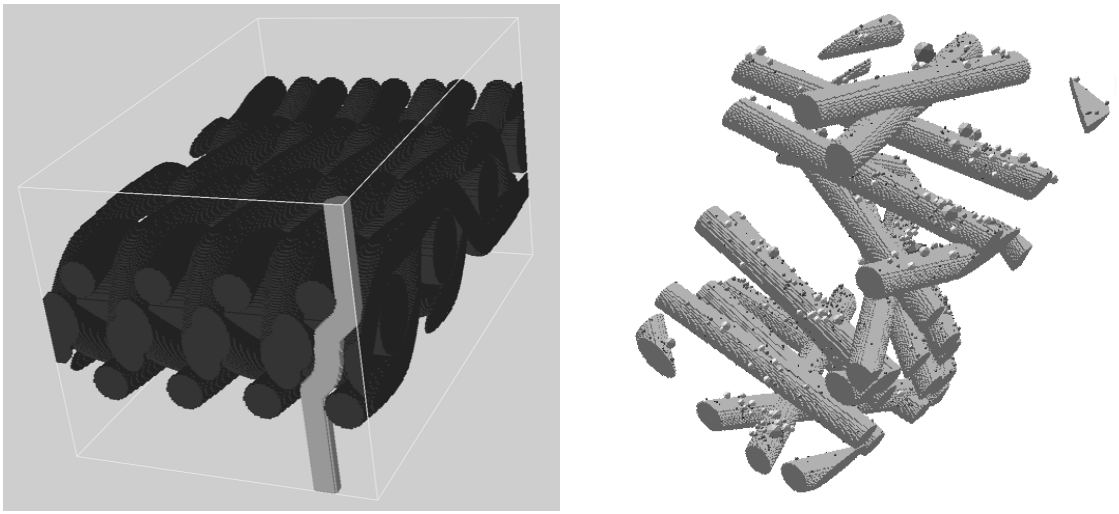

a) b)

Figure 9: Simulation of absolute filter fineness (a) and simulation of dust deposited on a fibrous filter (b).

3.1 *Fluid flow.* The standard description of fluid flow is by the Navier-Stokes equations. We consider purely viscous, incompressible fluids and stationary flows, so that there is no time-dependence. Conservation of momentum and conservation of mass can be written in the pressure – velocity formulation as follows:

$$-\mu\Delta\vec{u} + (\rho\vec{u}\cdot\nabla)\vec{u} + \nabla p = \vec{f}\text{ , (conservation of momentum)} \quad (1)$$

$$\nabla\cdot\vec{u} = 0\text{ , (conservation of mass)} \quad (2)$$

In equations (1) and (2) $\vec{u}$ is the fluid velocity, p is the pressure, is the fluid viscosity and $\vec{f}$ is a force density. Our standard procedure is to compute the velocity-field for a given pressure drop by converting the pressure drop into a force density and using periodic boundary conditions. When the mean velocity is prescribed, the pressure drop can be adapted until the desired mean velocity is reached.

The flows in most filter media are so slow that one may drop the inertia term from the Navier-Stokes equations to reach the Stokes equations. This is done because both the velocity and the gradient of the velocity are small, and the product of these two small terms is much smaller than all other terms in the equations.

$$-\mu\Delta\vec{u} + \nabla p = \vec{f}\text{ , (conservation of momentum)} \quad (3)$$

$$\nabla\cdot\vec{u} = 0\text{ , (conservation of mass)} \quad (4)$$

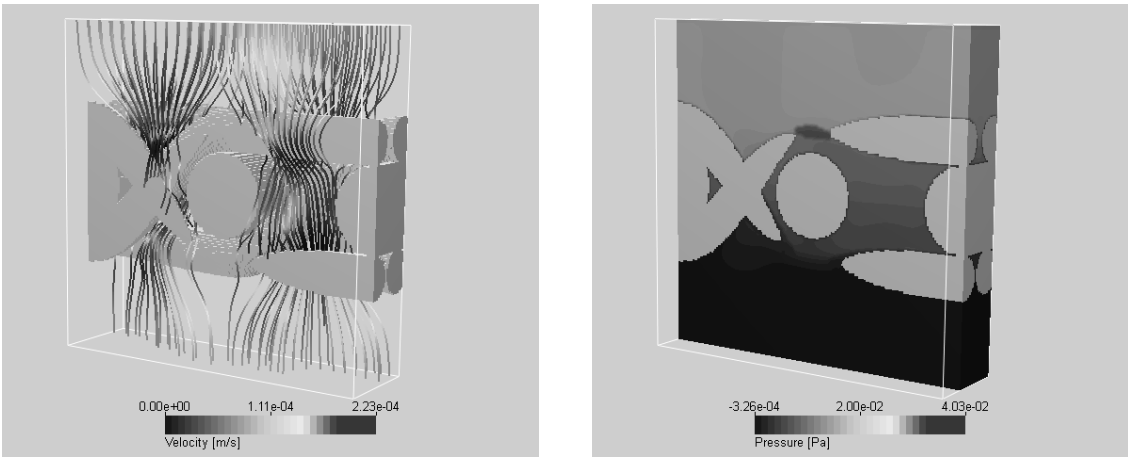

a) b)

Figure 10: Stream lines (a) and pressure (b) computed for the flow through a Dutch weave metal wire mesh.

When the scales of the particles are much smaller than the filter media, a third set of equations is used: the Navier-Stokes-Brinkman equations [9]. The additional term accounts for porous media formed by the sub-grid sized particles on the surfaces of the filter media. The equations couple the free flow in the pores with flow in porous media, which is usually descry bed by the Darcy equation.

$$-\mu\Delta\vec{u} + (\rho\vec{u}\cdot\nabla)\vec{u} + \mu K^{-1}\vec{u} + \nabla p = \vec{f}\text{ , (conservation of momentum)} \quad (5)$$

$$\nabla\cdot\vec{u} = 0\text{ , (conservation of mass)} \quad (6)$$

K^{-1} is the inverse of the permeability tensor and K^{-1} is the flow resistivity. In the empty cells, K^{-1} vanishes so that equation (5) becomes equation (3). In the porous cells, K^{-1} becomes quite large, and the velocity $\vec{u}$ small. In that regime, the velocity terms on the left of equation (5) may be neglected and we find Darcy's law

$$\vec{u} = -\frac{K}{\mu}(\nabla p - \vec{f})\text{ . (Darcy's law)} \quad (7)$$

By combining the equations for the unconstrained flow and flow in porous media, computations of filtration properties of cartridge filters (c.f. §2.5) and filter cakes (c.f. §2.6) become possible.

For the varying requirements of these sets of equations, a number of different solvers are in use. The ParPac Lattice-Boltzmann code [6] for all three sets of equations is very well parallelized and works on very large problems in resolved filter media on distributed memory machines. A finite volume code SuFiS (see [9] and [3]) also for all three sets of equations is designed for computations of complete filters, including the housing. Another class of finite volume codes, FFF-Stokes [17] solves only Stokes flow. However, it has the lowest memory requirements and fastest solution times for highly porous media.

There are several challenges for the computation of flow fields for resolved filtration simulations. The first is the need for an accurate geometric representation of the filter media and its translation into a computational grid. This challenge is met for a variety of structures as seen in §2. The structure is simply identical with the grid, different

from other approaches followed for example by Fluent®, CFX® and Star-CD®. Because the computational domains become very large, highly efficient codes in terms of memory and run-time are necessary. The regular behavior of the structure helps saving memory for coordinates, sophisticated new algorithms are used and the power of modern computers is utilized by parallel implementations. While the current state of the art for about 1,000 x 1,000 x 1,000 cell structures is sufficient for the prediction of the pressure drop and deposition of large particles, nano particles and nano fibers require even better resolved obstacle surfaces [22]. Hence, work on local grid coarsening is in progress to allow computations on 10,000 x 10,000 x 10,000 cell structures within the next couple of years.

3.2 *Electric charges.* In the current simplest model for fibrous filters [13], a prescribed charge is distributed equally on the fiber surfaces. A constant amount of charge ρ is assigned on each surface cell wall. A boundary value problem, the Poisson equation, is solved for the electric field :

$$\Delta u = \rho\chi(\partial\Omega) \quad : \text{ singular force Poisson equation} \tag{7}$$

$$\vec{\mathrm{E}} = \nabla u \quad : \text{the electric field} \tag{8}$$

The potential u is periodic in the x- and y-directions, and satisfies zero Dirichlet boundary conditions at a distance outside the filter media. By construction, these boundaries lie away from the fibers and there is no conflict between singular forces on fiber surfaces and the Dirichlet conditions. Due to the periodic boundary conditions, the potential feels a non-integrable amount of charges and tends to infinity as the Dirichlet boundary moves outwards. That is, the potential u depends on the location of the Dirichlet condition. But its derivative, the electrical field $\vec{E}$ remains almost independent of the location of the Dirichlet boundary as long as the boundary is sufficiently far away from the media.

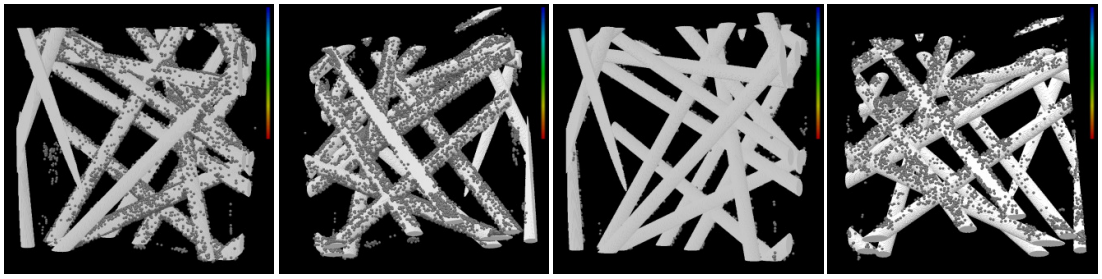

a) b) c) d)

Figure 11: Deposition on a fibrous media. Particles are started at random positions in a plane perpendicular to the flow direction and then transported to their deposition locations by (10) and (11), without charges on the fiber surfaces. a) front view, b) rear view. With charges on the surfaces c) front view and d) rear view. From [13].

The largest challenge for the computation of electric fields lies in the need for detailed statistics regarding the charge distribution on fiber surfaces. In terms of memory and time requirements, equations (7) and (8) are far less demanding than the Navier-Stokes equations, i.e. the latter dominate the computational effort. A very interesting future development will be the modeling and simulation of charge cancellation. This means the time dependent reduction of the electric field due to aging of the filter and due to charge neutralization when charged particles hit the fiber surfaces.

3.3 *Filter efficiency*. To simulate the filter efficiency, two effects must be modeled: The transport of the particle with the fluid flow, and the collisions and deposition of the particle with the filter media. Regarding transport, we assume highly dilute concentrations so that particles do not interact with each other while in flight. We also assume small and light particles, so that the change of the fluid flow due to the particles can be neglected. Particles are spherical so that their motion and collision computation is easy and quick. The choice of the particle diameter follows a given particle size distribution. To be statistically stable, for filter efficiency simulations it is important to use enough particles of each diameter. Relative numbers of particles sizes do not matter for filter efficiency computations because the particles do not interact in any way. Several thousand particles per diameter are usually sufficient. Particles are placed at random positions near the inlet of the flow region and then transported according to Newton's second law.

$$\vec{F} = m\vec{a}\,. \tag{8}$$

Here $\vec{F}$ is the force on the particle, m its mass and $\vec{a}$ the resulting acceleration. The particle moves under the influence of its own inertia, friction with the surrounding fluid and diffusion due to Brownian motion. An electric field in the filter media may exert an attractive or repulsive influence on the trajectory of the particle. Except for the inertial effect which is inherent to equation (9), all effects are viewed as coexisting forces. In this way, equation (9) becomes equation (10). Together, (10) and (11) form a system of stochastic ordinary differential equations for the motion of a particle.

$$\frac{d\vec{v}}{dt} = -\gamma(\vec{v}(\vec{x}(t)) - \vec{u}(\vec{x}(t))) + \sigma\frac{d\vec{W}(t)}{dt} + \frac{q\vec{E}(\vec{x}(t))}{m}\,, \tag{10}$$

$$\frac{d\vec{x}}{dt} = \vec{v}\,. \tag{11}$$

Here t means time, $\vec{x}$ space and $\vec{v}$ is the velocity of the particle. The first term on the right of equation (10) describes the friction between the particle and the surrounding fluid with γ as friction coefficient of a force that is proportional to the difference in velocity of the particle and the nearby fluid. For slowly moving, circular particles, γ is defined in equation (12).

$$\gamma = \frac{6\pi\mu R}{m}\,. \text{ (Stokes-friction)} \tag{12}$$

The radius of the particle is denoted by *R*. The second term in (10) describes Brownian motion by a three-dimensional Wiener process denoted by $\vec{W}$. *T* is the temperature and k_B is the Boltzmann constant. By Einstein's fluctuation-dissipation theorem, we have

$$\sigma^2 = \frac{2k_B\gamma T}{m}\,. \tag{13}$$

The third term on the right of equation (10) describes the influence of the electric field denote by $\vec{E}$ on the particle motion. Here *q* is the charge of the particle. The system (10) and (11) is solved by an implicit time-discrete Euler stepping method.

Besides the particle motion, also the particle deposition is critical for the simulation of filter efficiencies. Deposition requires the detection of collisions in every time step of tracking (10) and (11) and a model for the stickiness between particles and media. Collisions are found by considering the particle position, particle radius and of course,

the location of the solids belonging to the filter media. In case of a collision, the particles energy is compared with prescribed adhesion and restitution forces. If the particles energy is low enough, it will stick to the solid material. Otherwise, it bounces off with reduced energy and different direction. The extreme cases of this model are “caught on touch” and “sieving”. In the first case, adhesion is so strong that a particle always sticks, and in the second case a particle will never get filtered unless it gets geometrically caught in a pore that is too small to let it pass. The various filter effects are shown in Figure 12 (a).

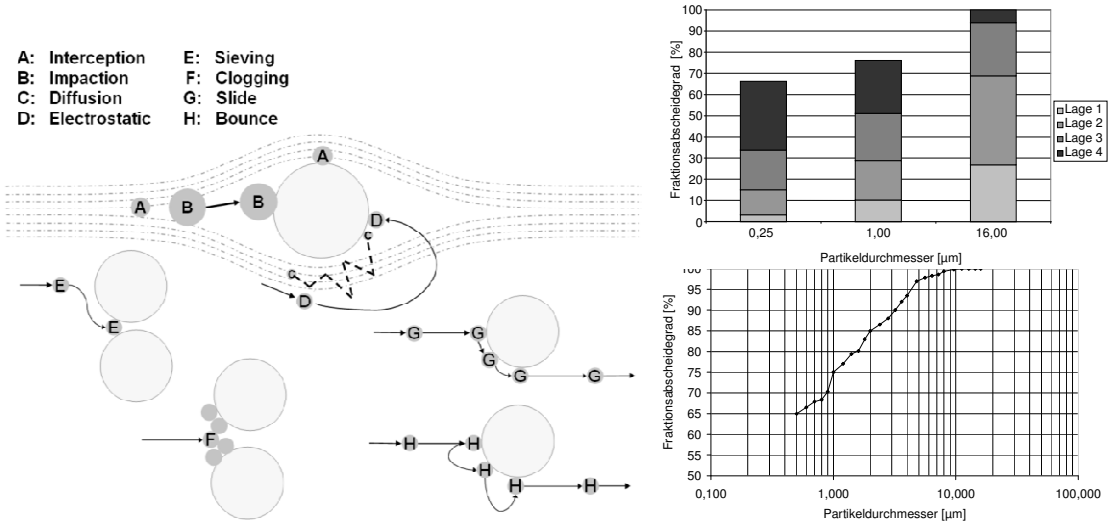

a) b)

Figure 12: a) Overview of filter effects. b) Filter efficiency for different particle diameters and 4 layers (fiber diameters decrease with layer index) and simulated filter efficiency for a general particle size distribution. From [11].

3.4 *Filter life time*. Filter life time simulation roughly speaking consists of iterating filter efficiency computations, namely flow simulations and particle transport and particle deposition. Some differences exist. For example, for life time computations, the relative amounts of particles must be according to the particle size distribution because particles now do interact with each other. After deposition, particles become obstacles or porous media in the next flow simulation, which may be accelerated by using the previously computed flow field. This also explains why the simulation produces increasing pressure drops – the flow is recomputed for a domain with fewer empty cells due to the deposited particles. So, between iterations the computational domain is modified. We stick to the uniform cubic cells and change some of them from empty to solid. With some we may associate a permeability, which changes the equations from Stokes or Navier-Stokes to Stokes-Brinkman or Navier-Stokes-Brinkman in those cells. Every originally empty cell knows about its degree of filling. If this value is bigger than zero, it means that at least one particle has deposited in the cell. In nano-mode (see Figure 6 a), assuming that particles are bigger than cells, the cell then becomes solid. In micro-mode, where particles are smaller than the cells, a cell can become partially filled. For such porous cell, the porosity is converted into permeability by formulas. The parameters for this relation may be computed in detailed computations in nano-mode [21]. Recently [12], the micro-mode was improved to not only remember the volume fraction covered by deposited particles, but also the precise location. The difference that this makes can be seen in Figure 12 – in b), the grid structure can be seen in the deposition patterns of the particles, while in d) this grid effect has disappeared. The sub-grid resolution for particles changes

also the rule how to convert porosity into permeability. One does not assume a uniform distribution of the particle mass over the cell, but can take into account that initially the mass is collected on one face of the cell.

Filter life time simulations are the most challenging both in terms of the modeling and the computations. Essentially, they rely on all other models and simulations and suffer from possible buildup in modeling errors as well as numerical errors. Yet, pressure drop evolution is one of the easiest macroscopically observable phenomena, and so discrepancies between simulation and reality are easily detected.

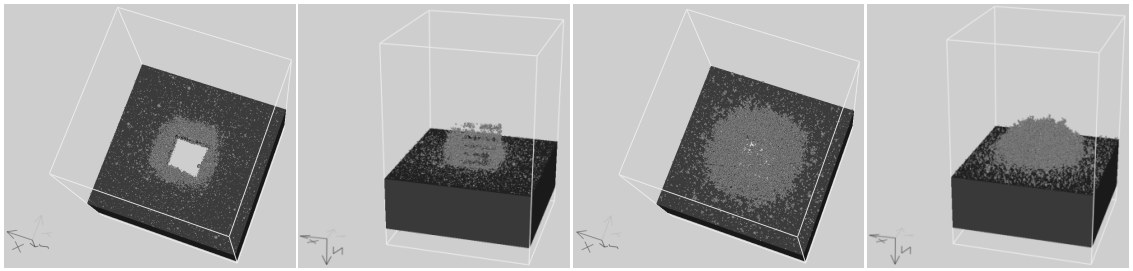

a) b) c) d)

Fig. 12: Soot layer computed with volume fraction model (a, b) and with sub-grid model (c, d) using a 16x16x23 grid with 1 micron resolution. From [15].

4. Conclusions and outlook

Filtration simulation benefits from the general trend that Computational Science and Engineering is a maturing field that some see as providing a third pillar to the scientific endeavor besides the established pillars theory and experiment. *The age of direct numerical simulation* or the *age of computing the details* is dawning. Today, computational experiments provide a way of *rapid prototyping* filtration applications and they are sure to lead to the derivation of new analytic descriptions for which the experimental derivation would simply have been too costly. Even if filter simulations do not always agree with experimental data, they provide invaluable detailed insights into filtration processes that help designing better filters and ultimately make our world more livable.

5. References

[1] J. Moscinski, M. Bargiel, Z. A. Rycerz and P. W. M. Jacobs, *The Force-Biased Algorithm for the Irregular Close Packing of Equal Hard Spheres*. Molecular Simulation, Vol. 3, No. 4, 1989, pp 201 – 212.

[2] J. Becker, A. Wiegmann and V.P. Schulz, *Design of Fibrous Filter Media Based on the Simulation of Pore Size Measures*, Filtech, Vol. I, 2007, pp 71-78.

[3] R. Ciegis, O. Iliev and Z. Lakdawala, On parallel numerical algorithms for simulating industrial filtration problems, Computational Methods in Applied Mathematics, Vol. 7, No. 2, 2007, pp 118-134.

[4] E. W. Dijkstra, *A note on two problems in connexion with graphs*, Numerische Mathematik, Vol 1, 1959, pp 269-271.

[5] A. Latz and A. Wiegmann, *Simulation of fluid particle separation in realistic three dimensional fiber structures*, Filtech, vol. I, 2003, pp 353-361.

[6] I. Ginzburg, P. Klein, C. Lojewski, D. Reinel-Bitzer, K. Steiner: *Parallele Partikelcodes für industrielle Anwendungen*, Verbundprojekt im Rahmen des

HPSC, Abschlussbericht, Fraunhofer Institut für Techno- und Wirtschaftsmathematik (ITWM) Kaiserslautern, März 2001.

[7] E. Glatt, S. Rief, A. Wiegmann, M. Knefel and E. Wegenke, *Struktur und Druckverlust realer and virtueller Drahtgewebe,* Filtrieren und Separieren, Vol. 23, No. 2, 2009, pp 61-65.

[8] M. Knefel, and P. Wirtz, *Auswahl und Optimierung technischer Gewebe mittels GeoDict, 2. Potsdamer FFT Fest- Flüssig Trennungstage, 2009.*

[9] O. Iliev, V. Laptev: *On Numerical Simulation of Flow through Oil Filters*, J. Computers and Visualization in Science, vol. 6, 2004.139-146.

[10] J. Ohser and F. Mücklich, *Statistical Analysis of Microstructures in Materials Science*, John Wiley & Sons, 2000.

[11] S. Rief, O. Iliev, D. Kehrwald, K. Steiner, A. Wiegmann and A. Latz, *Simulation und virtuelles Design von Filtermedien und Filterelementen,* Haus der Technik Fachbuch Band 75 *Filtration in Fahrzeugen*, Expert Verlag, 2006, pp 188-202.

[12] S. Rief, D. Kehrwald, K. Schmidt and A. Wiegmann, *Simulation of ceramic DPF media, soot deposition filtration efficiency and pressure drop evolution,* Proceedings of the 10th World Filtration Congress, Vol. III, 2008, pp 318-322.

[13] S. Rief, A. Latz and A. Wiegmann, *Research Note: Computer simulation of Air Filtration including electric surface charges in three-dimensional fibrous micro structures*, Filtration, Vol. 6, No. 2, 2006, pp 169-172.

[14] T. Saito and J.-I. Toriwaki, *New algorithms for Euclidean distance transformations of an n-dimensional digitized picture with applications,* Pattern Recognition, Vol. 27, 1994, pp. 1551-1565.

[15] K. Schladitz, S. Peters, D. Reinel-Bitzer, A. Wiegmann, J. Ohser, *Design of acoustic trim based on geometric modeling and flow simulation for nonwoven*, Computational Material Science, Vol. 38. No 1, 2006, pp 56-66.

[16] V. P. Schulz, P. P. Mukherjee, J. Becker, A. Wiegmann and C.Y. Wang, *Modelling of Two-Phase Behavior in the Gas Diffusion Medium of Polymer Electrolyte Fuel Cells via Full Morphology Approach*, Journal of the Electrochemical Society, Vol. 154, No. 4, 2009, pp B419-B426.

[17] A. Wiegmann, *Computation of the permeability of porous materials from their microstructure by FFF-Stokes*, Berichte des Fraunhofer ITWM, Nr. 129, 2007.

[18] A. Wiegmann, *GeoDict*, Fraunhofer Institut für Techno- und Wirtschaftsmathematik, http://www.geodict.com, 2009.

[19] A. Wiegmann, L. Cheng, E. Glatt, O. Iliev and S. Rief, *Design of pleated filters by computer simulations*. Berichte des Fraunhofer ITWM, Nr. 155, 2009.

[20] A. Wiegmann, S. Rief and D. Kehrwald, *Computational Study of Pressure Drop Dependence on Pleat Shape and Filter Media*, Filtech, Vol. I, 2007, pp 79-86.

[21] A. Wiegmann, S. Rief and A. Latz, *Soot Filtration Simulation - Generation of Porous Media on the Micro Scale from Soot Deposition on the Nano Scale,* Proceedings of the 2nd European Conference on Filtration and Separation, Compiegne, France, 2006, pp 141-147.

[22] A. Wiegmann, K. Schmidt, S. Rief, L. Cheng and A. Latz, *Simulation studies of deposition mechanisms for aerosol particles in fibrous filters including slip flow,* 10th World Filtration Congress, Vol. III, 2008, pp 127-131.